DROPLET BREAKUP ENERGIES AND FORMATION OF ULTRA-FINE MIST

K.C.Adiga
NanoMist Systems, LLC
151 Osigian Blvd, Suite 199, Warner Robins, GA 31088.
Voice: 478-953-2709 Email: kcadiga@nanomist.com
And

Heather D. Willauer, Ramagopal Ananth, and Frederick W. Williams
The Navy Technology Center for Safety and Survivability
Chemistry Division, Naval Research Laboratory
Washington D.C. 20375-5320

SUMMARY

The aerodynamic droplet breakup process in water spray blast mitigation is an attractive beneficial feature for blast mitigation technology development. This blast-induced droplet breakup occurs due to local acceleration of the gas and the coarse water droplet acceleration. The droplet breakup dominates when the relative velocity between the gas and droplet develop, so that the droplet Weber number is more than 12 for a sufficient time. The process has been demonstrated in reduced scale experiments as well as in limited large-scale tests.

The overall objective pf the project is to identify and understand the mechanisms by which water mist mitigates overpressures associated with blasts. This knowledge can be used to optimize and engineer future Navy ship-wide water mist systems having the capability of acting as both a fire suppression system and a blast mitigation system. This work was focused on assessing the implications of blast-induced droplet breakup and the droplet evaporation processes on the energy extraction and weakening of the shock.

Droplet breakup energies were determined from the surface energies of both parent and child droplets. Breakup energy of 18 j/kg was required to fragment a 0.5 mm parent droplet into 10,000 mono-dispersed 20 μm droplets. This energy would be extracted by the shock front. When the droplet breakup energy was compared to the vaporization energy of 1 kg of water (2.5 $x10^6$ j/kg); its energy extraction did not appear significant in weakening the shock. While the droplet deformation energy and curvature effects could increase the breakup energy, its overall contribution to the total energy extraction was not as significant as the vaporization enthalpy. The analysis found a tremendous increase in the droplet vaporization rate with the 22-fold increase in surface area of the 20 μm child droplets. The surface to volume ratio of the ultra fine droplets and their vaporization time scales indicate they should be well positioned for shock energy extraction. Thus, the study revealed that the droplet breakup process forming ultra fine water mist has significant impact on the blast mitigation process.

1.0 INTRODUCTION

The US Navy has recognized the benefits of water mist for fire suppression [1,2], and as a result these systems have been installed in the Navy's latest class of amphibious ships, the *San Antonio* class (LPD-17). As these systems are being included in more ship designs, there is a desire to investigate their potential use in limiting the primary damage area (PDA) caused by an explosion from a weapon or terrorist attack [3-5].

Many reports have cited mitigation of condensed-phase explosions and vapor cloud explosions using water mist and a few have addressed some of the plausible mechanisms by which mitigation was achieved [3,5]. These include the extraction of energy from both the shock front and the chemical reaction zone when water droplets fragment and evaporate [3,5]. The water mist droplet size and concentration, the chemical composition of the explosive (missile, TNT, dust cloud), and the geometric complexity of the area being mitigated determines how well the water droplet interaction promotes energy absorption and thus mitigation.

Ideally a shipboard water mist system would mitigate the initial blast overpressures and any quasi-static overpressures and secondary effects caused by a blast. Shipboard environments are geometrically complex, consisting of multiple compartments ranging in size and containing varying degrees of congestion. A few reports suggest that a blast in this type of environment could actually enhance the overpressures due to the reflection of shock waves [3]. The other issues are the time, the amount of water, and water droplet size needed to achieve mitigation in the event of an incident.

The Naval Research Laboratory (NRL) was sponsored by the Office of Naval Research (ONR) to study these issues by conducting a series of small scale blast mitigation tests in the summer of 2005 [6]. The tests were carried out in a bombproof shelter at the Naval Surface Warfare Center (NSWC), Indian Head, Maryland using (2 lbs, 5 lbs, and 7 lbs) TNT. The studies showed that the water mist reduced the quasi-static overpressures by as much as 47% [6]. The mist characterization studies indicated the water droplet size used for mitigation ranged from (35 - 550 μm) with a Sauter Mean Diameter (SMD) greater than 50 μm [7]. SMD is the diameter of the droplet whose surface to volume ratio is equal to that of the entire spray [8].

The results of the blast mitigation studies suggest there are other mechanisms, in addition to water droplet fragmentation and evaporation [3,5], by which water mist mitigates the blasts. We propose a comprehensive set of mechanisms of interactions. Figure 1 shows a schematic of the proposed interaction of water droplets in the detonation process. The water mist (parent droplets) is essentially unaffected by the incoming shock wave. Once the front has passed, the droplets enter an environment where the air is moving at supersonic velocities. These forces shear the coarse parent droplets into smaller droplets (child droplets) and energy is absorbed from the shock front. The child droplets produced can interact with the shock front, the reaction front, and the reaction product zone (Figure 1) by other mechanisms in addition to evaporation to absorb energy from the blast.

Behind the shock front, the small droplets are rapidly accelerated to shock velocity absorbing kinetic energy from the blast as there is a transfer of momentum from the gas phase to the water

phase. When the droplets penetrate the reaction front, they can absorb radiation and evaporate, causing further weakening of the blast. If the droplets reach the reaction products zone, more evaporation may occur resulting in slowing down the expansion process.

Blast-induced droplet breakup is just one of the mechanisms in which energy is absorbed from the shock and it is clear the efficiency of this process is critical to producing child droplets capable of penetrating the different blast zones to achieve mitigation by latent heat and kinetic energy absorption. The energy absorption and time scales associated with the droplet breakup process are significant to developing an understanding of the mechanisms involved in water mist blast mitigation.

The chemical composition of high explosives and its amount determine the time scales for the shock and reaction front propagation. Water mist droplet size plays a key role in determining the time scales for droplet breakup, momentum transfer, evaporation, and radiation absorption. Therefore, optimum droplet size and concentration depend on the composition and quantity of high explosive used in a given compartment size.

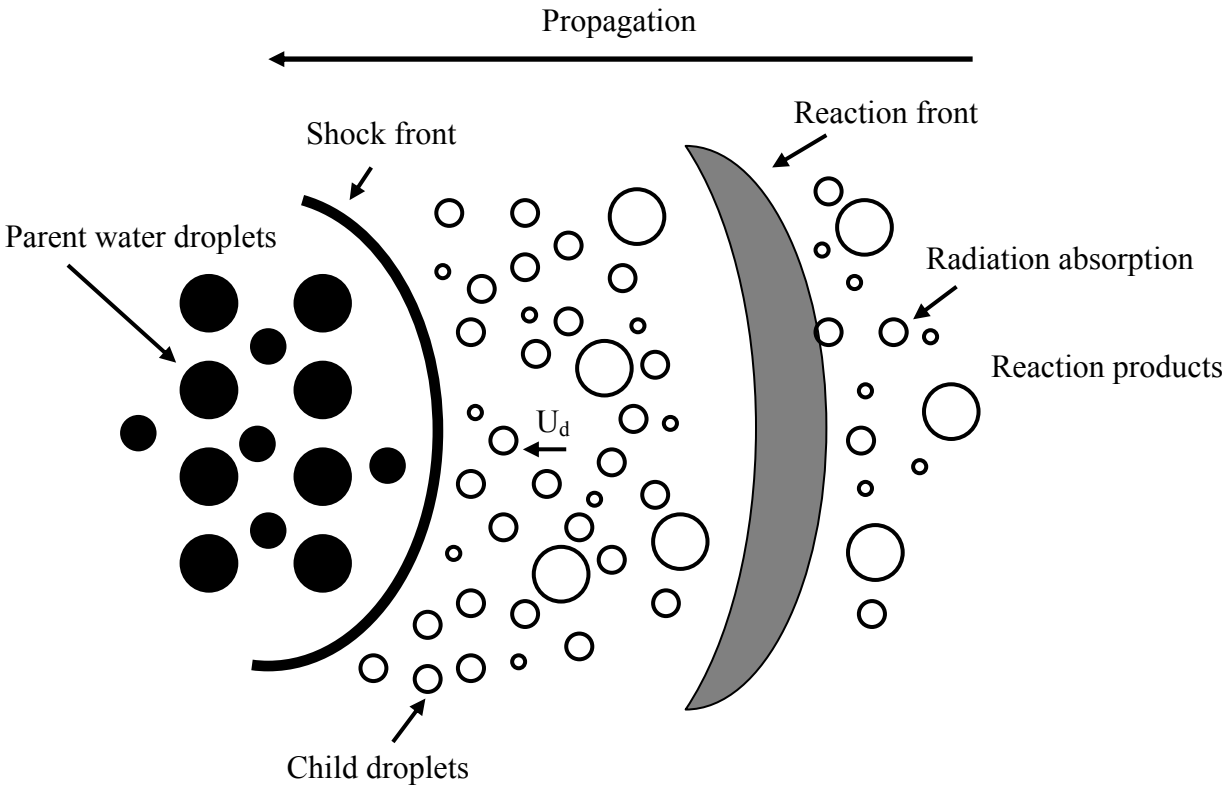

Figure 1: Interaction of water droplets in detonation process

2.0 BACKGROUND

The aerodynamic droplet breakup process in water spray blast mitigation is an attractive beneficial feature for technology development. This blast-induced droplet breakup occurs due to local acceleration of the gas and the coarse water droplet acceleration. The droplet breakup dominates when the relative velocity between the gas and droplet develop, so that the droplet Weber number is more than 12 for a sufficient time [3,9-14]. The process has been demonstrated in reduced scale experiments as well as in limited large-scale tests.

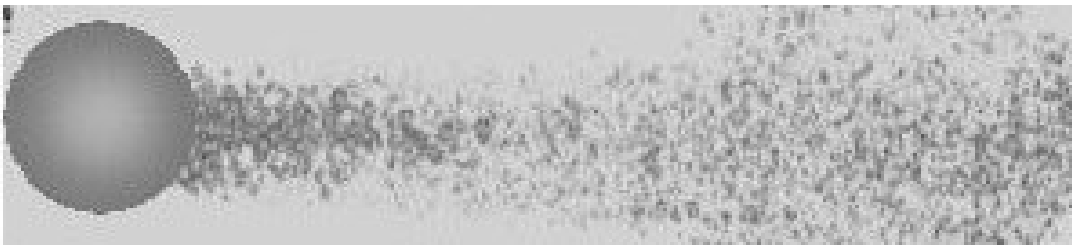

Figure 2: Droplet breakup process in an accelerating flow field; We > 12

The Weber number is:

$$We = \rho V^2 D/\sigma \qquad (1)$$

In this equation, ρ is the density of the flow field, V is the initial relative velocity between the flow field and the drop, D is the initial diameter of the drop and σ is the surface tension of the liquid. The mechanism of droplet fragmentation depends on the Weber number of the parent droplet. The mechanistic pathways to final child droplets generally observed for droplets in the gas flow field are listed below:

- Vibration breakup We < 12
- Bag breakup 12 < We < 50
- Bag-and-stamen breakup 50 < We < 100
- Sheet stripping 100 < We < 350
- Wave crest stripping followed by catastrophic breakup We > 350

A schematic of this mechanism is shown and described by Pilch and Erdman [14].

As shown in Figure 2, a coarse precursor droplet of 1-5 mm (1000-5000 μm) is fragmented into 20-30 μms. The fragmentation efficiency is dependent on the droplet flow rate and initial droplet size and concentrations. The ultra fine mist (UFM) (child droplets) formed by the breakup process is a powerful blast mitigation agent. Undoubtedly, the vaporization energy by the ultra fine water mist is one of the sources of energy extraction from the shock. This analysis evaluates the time scales and relative contributions these two processes have on weakening the shock.

3.0 OBJECTIVES

The objective of this work is to identify and understand the mechanisms by which water mist mitigates overpressures associated with blasts. This knowledge can be used to optimize and engineer future Navy ship-wide water mist systems having the capability of acting as both a fire suppression system and a blast mitigation system. This report specifically assesses the blast-induced droplet breakup process and the droplet evaporation process to determine the energy extraction significance these processes have on weakening the shock.

4.0 RESULTS

4.1 Analysis of Breakup Process and Computing Energies

First, a simple droplet breakup process, without referring to mechanisms, is shown schematically in Figure 3 in terms of initial and final states. In this simple schematic, the droplet first deforms and elongates under flow-induced stress. This initial state (State 1) and the final state (State 2) are related to the droplet's properties such as diameter, surface area, and surface energies, as shown in Figure 3.

As a first approximation, the energy associated with the breaking of a single droplet into several child droplets will be computed based on the surface energy difference between State 1 and State 2. There is a formation route or path in between these two states. For example, before the droplet breaks up, the drops deform and reach an ellipsoidal shape similar to that of an oblate spheroid. Such a mechanistic pathway imposes an activation route with an energy barrier to pass through before coming to State 2. The implication of this will be reviewed and an order of magnitude analysis will be provided later in the report.

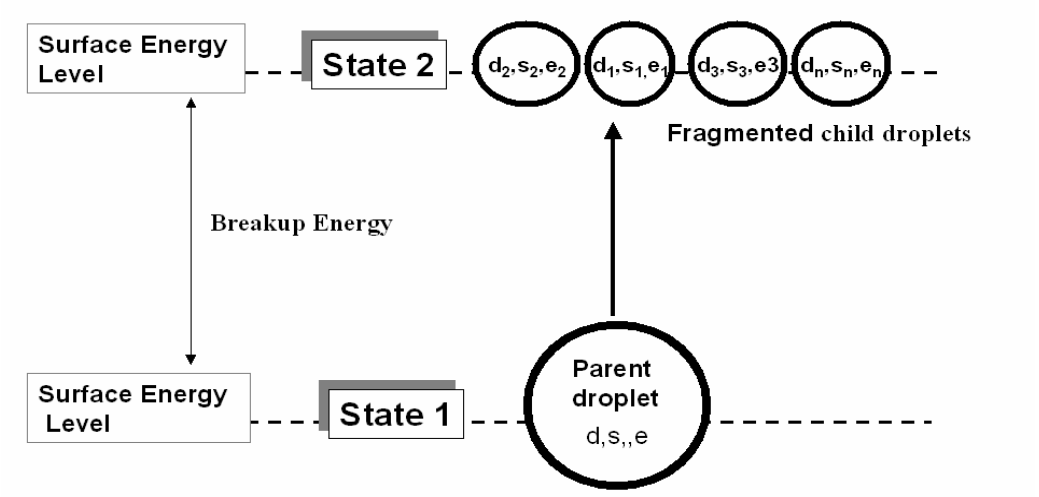

Figure 3: Various surface energy states for droplet breakup into child droplets

Under favorable conditions, the initial droplet will break into a larger number of child droplets behind the shock wave. During the breakup process, there will be a considerable increase in surface area per unit mass of child droplets that in turn will have increased droplet surface energy. The droplet surface energy is computed using the droplet surface area and surface tension of water as follows:

Surface area of a parent droplet of mass m, and diameter, d:

$$Sp= \pi d^2 \tag{2}$$

State 1: Surface energy of parent droplet of diameter

$$Ep=\pi d^2 \sigma \tag{3}$$

where σ is the surface tension of water.

The total surface area, S of child droplets of total mass m and diameters d_1, d_2, d_3..d_n (m):

$$S= \pi(d_1^2+ d_2^2+\ldots\ldots d_n^2) \tag{4}$$

State 2: Total surface energy of child droplets of total mass, m (kg):

$$E_c=\pi\sigma\ (d_1^2+ d_2^2+\ldots\ldots d_n^{2)} = S\sigma \tag{5}$$

The surface energy difference between the final state (State 2) and the initial state (State 1) per unit mass (Eqs. 3 and 5):

$$\Delta E = (Ec-Ep)/m\ (j/kg) \tag{6}$$

This is the energy required to break the parent droplet into "n" number of child droplets per unit mass of droplet.

Results are shown in Figure 4 for a parent (initial) droplet with a 500 μm diameter (0.5 mm) (corresponding to 6.54 x 10^{-8} kg) breaking up into ~10,000 child droplets. Here, the cascading breakup effects are not considered, namely the parent droplet directly goes to a child droplet as opposed to intermediate stages which are not shown.

Figure 4 also shows how the diameter of the child droplets decreases as a function of the number of fragments formed. For about 10,000 fragments, the final droplet size is close to ~23 μm. These are mono-disperse droplets. Calculations can be done using Monte Carlo methods for a wide range of droplet size distributions. However, this approach is not considered here since, for the calculation of surface energy, all that matters is the total surface area of the final droplets. The droplet fragments formed are just in the right size range for blast and mitigation to occur by rapid energy extraction by UFM.

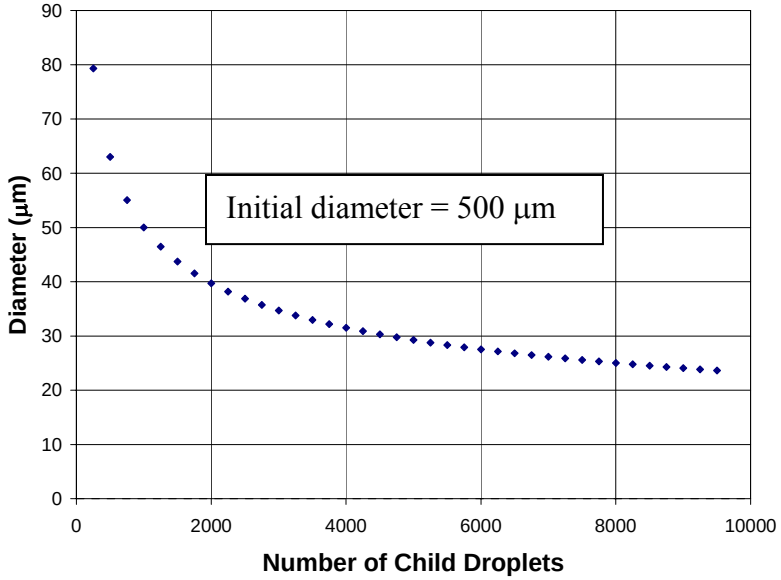

Figure 4: Diameter of child droplets as a function of number of fragments formed

Figure 5 shows how the surface area per unit mass increases as a function of the total surface area per unit mass of the child droplets. The initial surface area of the parent droplet is 12 m^2/kg, and upon its fragmentation, 260 m^2/kg of child droplets are formed. This 22-fold increase in surface area of ~23 μm mono-dispersed UFM, will increase the surface energy of droplets as well as their vaporization rates. The increase in surface area will have two immediate implications: 1) an increase in the surface energy of the child droplets that will be absorbed by the shock causing more energy extraction and possible weakening of the shock, and 2) rapid vaporization of UFM absorbing 2.5x 10^6 j/kg of water.

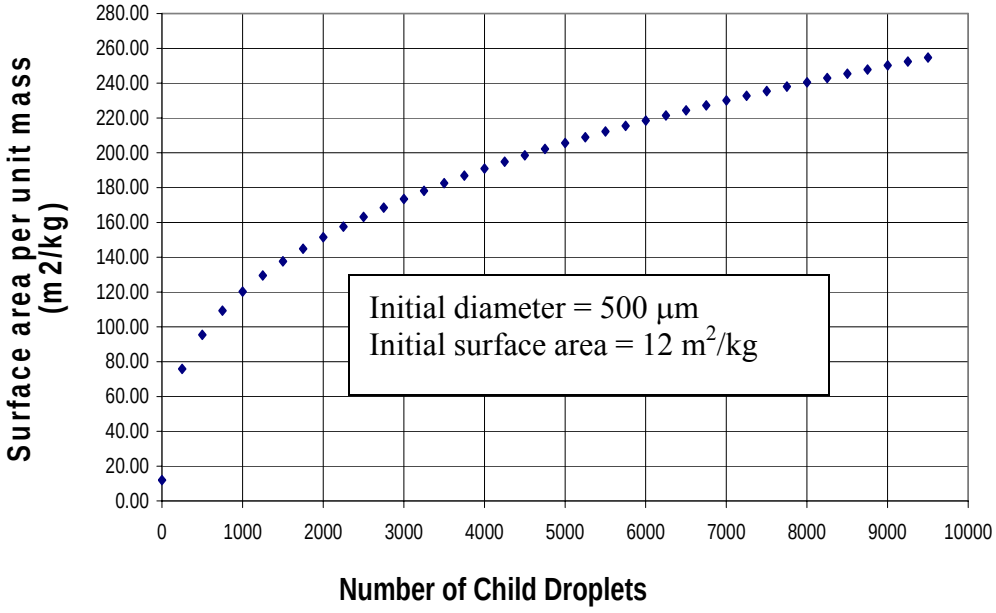

Figure 5: Variation of surface area as a function of number of droplets

Figure 6 shows the surface energies of fragmented droplets, and how it is increased from 0.88 to 18.5 j/kg for 10,000 droplets.

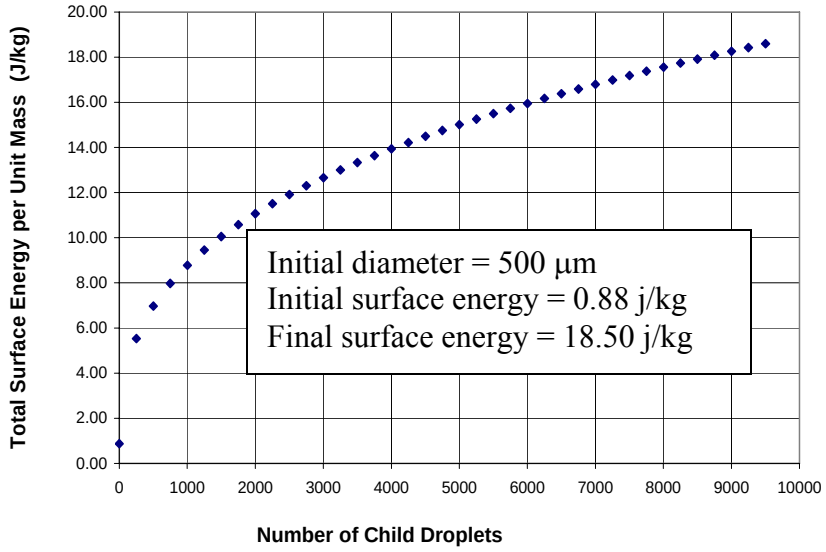

Figure 6: Surface energy variation with number of child droplets

This increase in surface energy results from the new surfaces created by the child droplets. This energy has to come from the shock wave. The difference in energies of the parent and the child droplets is shown in Figure 7.

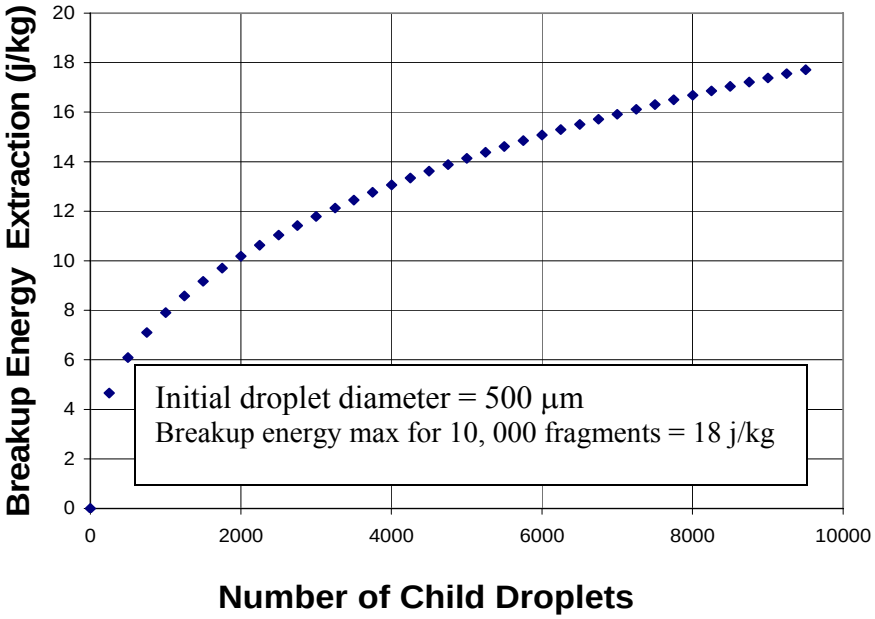

Figure 7: Breakup energy variation with number of child droplets

This is the net energy to be extracted from the shock to break the parent droplets. This energy extraction, if significant, could weaken its strength. The total energy extraction is approximately 18 j/kg (liter) when the coarse water spray droplets are fragmented into UFM. This magnitude is small compared to the energy extraction by vaporization of 1 liter of water (2.5 $x10^6$ j/kg). Thus, the energy budget clearly indicates that the contribution from the breakup process, as compared to latent heat absorption, is not significant. The fragmentation of the parent droplet is however very important to the global process. The increase in surface area created by the child droplets will enhance shock energy extraction by reducing the vaporization time scales.

4.2 Deformation Transition Energy Consideration in Breakup Process Path

Based on the energy extraction possibilities presented, the magnitude of the droplet breakup energy is far less effective compared to enthalpy of vaporization of water. The breakup energy is based on the computed surface energy difference between State 1 (parent droplet) and State 2 (child droplets). However, the droplets must transition through an energy barrier before reaching their final state. For example, when a completely spherical droplet is subjected to the flow field, its windward side will have higher pressure compared to the forward stagnation point. Figure 8 shows a schematic of energy states for parent droplet, child droplets, and the intermediate activation process of deformation.

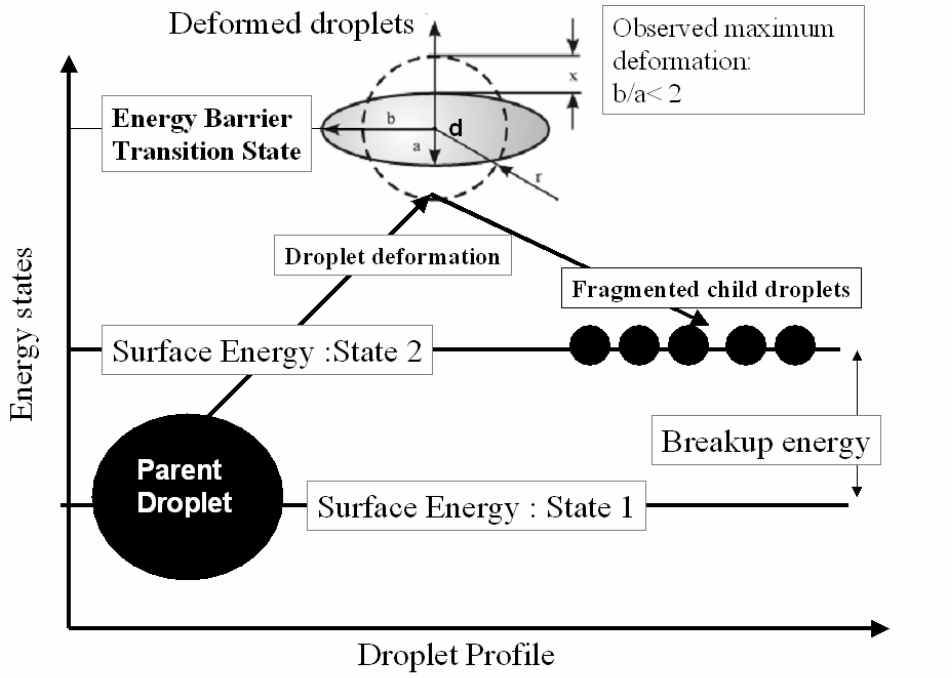

Figure 8: A schematic of activation process of droplet deformation before reaching the final child droplet stage

The droplets first deform into ellipsoid shapes as shown in Figure 9 before they go through several of the mechanisms illustrated and described by Pilch and co-workers [14]. In the vibrational type shown for a low Weber number (We < 12), droplets start necking in and break into two droplets after becoming ellipsoid. This curvature effect will push the surface energy to

a higher state before fragmentation occurs, leading to additional energy absorption. This process is not considered important because the Weber number encountered in the detonation field must be higher.

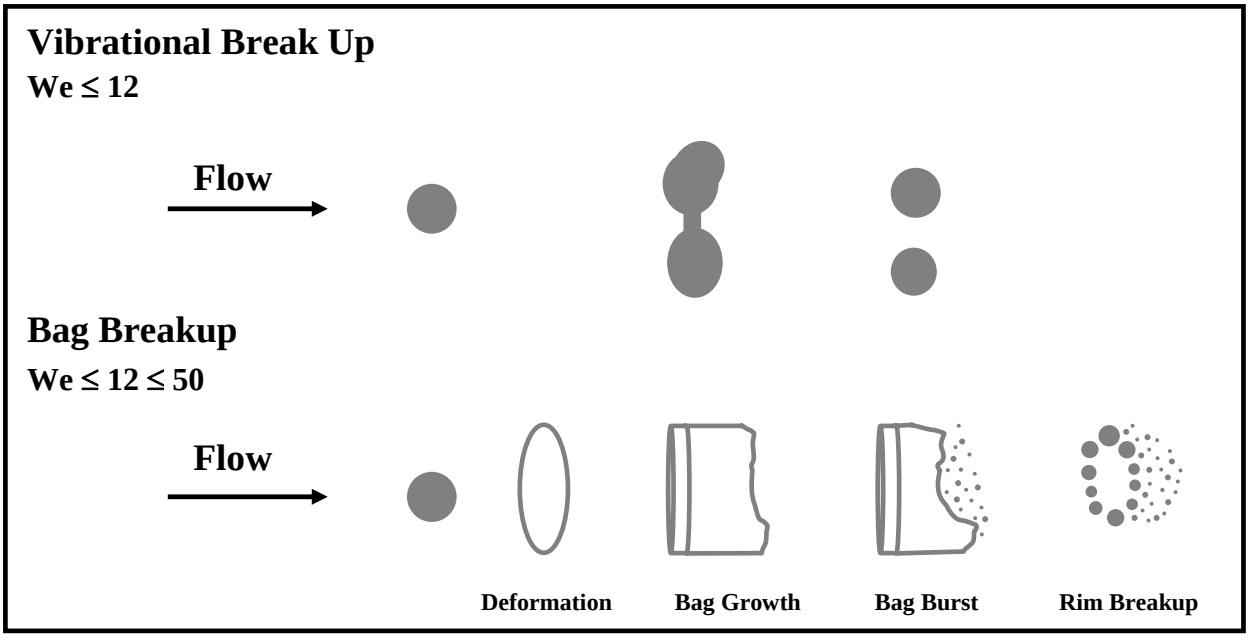

Figure 9: Breakup mechanisms

Referring to the bag breakup process described by Pilch [14] and illustrated in Figure 9, there is a significant curvature effect, as the surface goes through ellipsoid and bag. The deformation will add additional surface area. Before the droplet breaks up, the drops deform and reach an ellipsoidal shape, similar to that of an oblate spheroid as shown in Figure 9.

Chryssakis and Assaniss have published descriptions of high Weber number droplet breakup with various deformation profiles for droplets undergoing fragmentation [12]. Hslang and Faeth [13] conducted experiments in a wide range of conditions and showed that the maximum drop distortion can be expressed as:

$$d_c/d = 1 + 0.19\ We^{1/2} \qquad \text{Oh} <;\ We < 100 \qquad (7)$$

where Oh is the Ohnesorge number incorporating the viscosity effects. However, when $We >$ 100, typical of detonation conditions, the

$$d_c/d \sim 2 \qquad \text{Oh} <;\ We > 100 \qquad (8)$$

As shown, the diameter increases to twice the original, but the other diameter also varies. This indicates that the surface area variation and the curvature effects before they fragment will not be

significant considering the initial (State 1) and final state (State 2) of a huge number of child droplets. This still is an insignificant amount of energy addition compared to the vaporization energy, which is 2.5 x 10^6 j/kg of water.

4.3 Energy Extraction by Vaporization of Fragmented Droplets and the Time Scales

The next aspect to be evaluated is the vaporization time scales of these fragmented droplets. For a qualitative judgment of the relative estimate of the droplet size effect on the vaporization behavior, the d^2-law droplet evaporation calculation will be used here. This expression does not consider the effects of the coupled flow field, heat transfer, residence time and the background humidity level (RH %).

The evaporation time, assuming dry air (Relative Humidity - RH = 0%) is given by :

$$t_{VAP} = \frac{D_{0,initial}^2 \ \rho_{liq}}{8\Gamma_{VAP} \ln\left(1 + \frac{m_{VAP,0} - m_{VAP,\infty}}{1 - m_{VAP,0}}\right)}$$

Where:

$m_{H_2O} = 0.0075$ for saturated air at 10^0 C and 1 atm

$$\tau_{H_2O} = 2.6 \cdot 10^{-5} \ \frac{kg}{m\ s}$$

$$\rho_{LIQ} = 1000 \frac{kg}{m^3}$$

$$t_{VAP} = \frac{D_{0,initial}^2 \rho_{LIQ}}{8\Gamma_{VAP} \ln\left(1 + \frac{m_{VAP,0} - m_{VAP,\infty}}{1 - m_{VAP,0}}\right)}$$

The droplet vaporization time scales as a function of droplet fragments from 0.1 μm to 500 μms are shown in Figure 10. Note that the droplet vaporization time scales start at microseconds for nearly μm-sized droplets and increase to minutes for coarse droplets of 0.5 mm (500 μm). It is expected these time scales will be much shorter, at high temperatures (in excess of 2000 ^{O}C) encountered in shock front. However, because of very high velocity, the residence time will be very short. Then, only droplets with vaporization time scales of microseconds or shorter will respond to shock energy extraction. The droplets of ultra fine mist (below 20 μm) will exhibit time scales of microseconds at those temperatures.

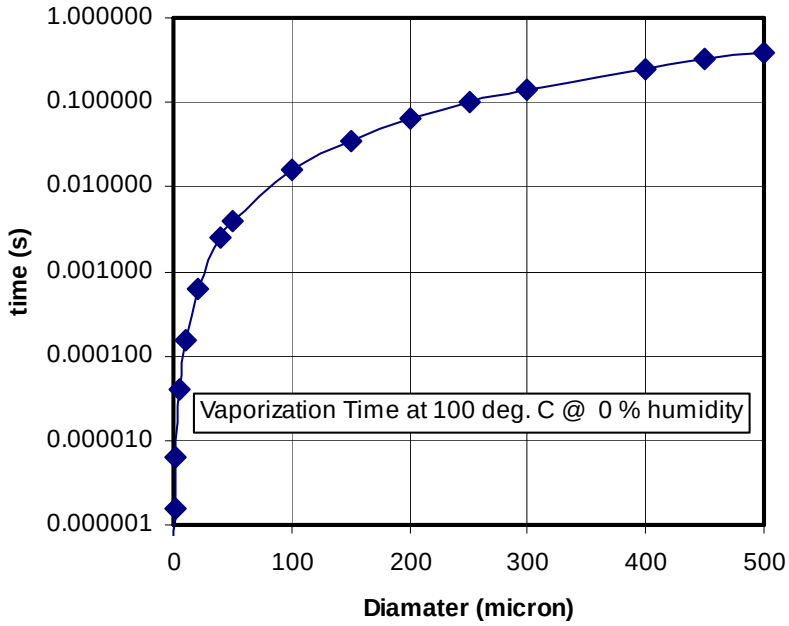

Figure 10: d^2-law evaporation time scales of child droplets from the shock-induced droplet breakup process

The analysis indicates that UFM (below about 20 μm) formed during the breakup process will be well positioned to extract the energy from the shock by vaporization in terms of closely matching microsecond time scales. As seen, the time scales for coarse droplets are approximate seconds; these droplets may contribute very little to the mitigation process if they are not fragmented. Based on the residence time scaling by the CFD modeling study, we find that even 100 μm droplets are not very well positioned for extracting energy by vaporization efficiently, since the residence time and vaporization time scales together will not match shock induced vaporization. Unfortunately, these medium scale droplets of 100 μm will not be fragmented because the Weber number will be much lower compared to 12.

5.0 CONCLUSIONS

Droplet breakup energies were determined from the surface energies of both parent and child droplets. A breakup energy of 18 j/kg was required to fragment a 0.5 mm parent droplet into 10,000 mono-dispersed ~23 μm droplets. This energy would be extracted by the shock front. When the droplet breakup energy was compared to the vaporization energy of 1 liter of water (2.5×10^6 j/kg); its energy extraction did not appear significant in weakening the shock. While the droplet deformation energy and curvature effects could increase the breakup energy, its overall contribution to the total energy extraction was not as significant as the vaporization enthalpy. The analysis also found a tremendous increase in the droplet vaporization rate with the 22-fold increase in surface area of the ~23 μm child droplets. Thus the surface to volume ratio of the ultra fine droplets and their vaporization time scales indicate they should be well positioned for shock energy extraction.

ACKNOWLEDGEMENT

This work is funded as part of the Office of Naval Research (ONR) Shipboard Fire Mitigation Thrust program.

REFERENCES

1. Back, G. G.; DiNenno, P. J.; Leonard, J. T.; Darwin, R. L. "Full Scale Tests of Water Mist Fire Suppression Systems for Navy Shipboard Machinery Spaces: Phase I – Unobstructed Spaces," NRL Memorandum Report 6180-96-7830, 8 March 1996.

2. Back, G. G.; DiNenno, P. J.; Leonard, J. T.; Darwin, R. L. "Full Scale Tests of Water Mist Fire Suppression Systems for Navy Shipboard Machinery Spaces: Phase II – Obstructed Spaces," NRL Memorandum Report 6180-96-7831, 8 March 1996.

3. Kailasanath, K.; Tatem, P. A.; Williams, F. W.; Mawhinney, J. "Blast Mitigation Using Water-A Status Report," NRL Memorandum Report 6410-02-8606, 15 March 2002.

4. Schwer, D.; Kailasanath, K. "Blast Mitigation by Water Mist (1) Simulation of Confined Blast Waves," NRL Memorandum Report 6410-02-8636, 16 August 2002.

5. Schwer, D.; Kailasanath, K. "Blast Mitigation by Water Mist (2) Shock Wave Mitigation Using Glass Particles and Water Droplets in Shock Tubes," NRL Memorandum Report 6410-02-8658, 21 January 2003.

6. Bailey, J. L.; Lindsay, M. S.; Schwer, D. A.; Farley, J. P.; Williams, F. W. "Blast Mitigation Using Water Mist," NRL Memorandum Report 6180-06-8933, 18 January 2006.

7. Willauer, H. D.; Bailey, J. L.; Williams, F. W. "Water Mist Suppression System Analysis," NRL Letter Report 6180/0030, 7 February 2006.

8. Lefebvre, A. H. "Atomization and Sprays," Hemisphere Publishing Corporation: Philadelphia, 1988.

9. Thomas G. O. On the Conditions Required for Explosion Mitigation by Water Sprays *Process Safety and Environmental Protection: Trans. Ins. Chem. Eng. Part B.*, 2000, 78, 339.

10. Temkin, S; Mehta, H. K. Droplet Drag in an Accelerating and Decelerating Flow. *J. Fluid. Mech.* 1982, 116, 297.

11. Brenton, J. R.; Thomas, G. O. Small-Scale Studies of Water Spray Dynamics During Explosion Mitigation Tests, *I. CHEM. E. Symposium Series No. 134, Hazards XII*, 1994, 39, 393.

12. Chryssakis, C. A.; Assaniss, D. N. "A Secondary Atomization Model for Liquid Droplet Deformation and Breakup under High Weber Number Conditions," ILASS Americas, 18th Annual Conference on Liquid Atomization and Spray Systems, Irvine, CA, May 2005.

13. Hslang, L. –P; Faeth, G. M. Near-Limit Drop Deformation and Secondary Breakup, *Int. J. Multiphase Flow*, **1992**, 18, 635.

14. Pilch, M.; Erdman, C.A Use of Breakup Time Data and Velocity History Data to Predict the Maximum Size of Stable Fragments for Acceleration-Induced Breakup of a Liquid Drop," *Int. J. Multiphase Flow*, **1987**, 13, 741.